Genes & Diseases (2022) 9, 741–752

Available online at www.sciencedirect.com

ScienceDirect

journal homepage: http://ees.elsevier.com/gendis/default.asp

FULL LENGTH ARTICLE

# The mevalonate pathway promotes the metastasis of osteosarcoma by regulating YAP1 activity via RhoA

**Xing Du, Yunsheng Ou, Muzi Zhang, Kai Li, Wei Huang, Dianming Jiang***

*Department of Orthopedics, The First Affiliated Hospital of Chongqing Medical University, Chongqing 400016, PR China*

Received 21 August 2020; received in revised form 21 October 2020; accepted 16 November 2020
Available online 21 November 2020

**KEYWORDS**
Metastasis;
Mevalonate pathway;
Osteosarcoma;
RhoA;
YAP1

**Abstract** Osteosarcoma is the most common malignant bone tumour, and the metastasis of osteosarcoma is an important cause of death. Evidence has shown that the mevalonate pathway is highly activated and is expected to be a new target for tumour therapy. In this study, we investigated the effect of mevalonate signalling on osteosarcoma metastasis and its molecular mechanism. First, we found that the key rate-limiting enzyme of mevalonate signalling, 3-hydroxy-3-methylglutaryl-CoA reductase (HMGCR), was highly expressed in osteosarcoma cells, and inhibition of HMGCR with simvastatin significantly inhibited the motility of 143B cells. Next, we found that YAP1 activity was significantly upregulated in osteosarcoma cells and that YAP1 knockdown inhibited the motility of 143B cells. We also found that the mevalonate pathway regulated the motility of 143B cells by modulating YAP1 phosphorylation and cellular localization. Moreover, we found that the activity of YAP1 was regulated by the mevalonate pathway by modulating the cell membrane localization of RhoA. Finally, we demonstrated that inhibition of the mevalonate pathway notably reduced the lung metastasis of 143B cells, as reflected by the decreased incidence and number of metastatic nodules and the increased survival time of the nude mice. Taken together, our findings suggest that the mevalonate pathway can promote the metastasis of osteosarcoma by activating YAP1 via RhoA. Inhibition of the mevalonate pathway may be a promising therapeutic strategy for osteosarcoma metastasis.


* Corresponding author. No.1 YouYi Road, Yu Zhong District, Chongqing 400016, PR China.
*E-mail address:* jdm201296@hospital.cqmu.edu.cn (D. Jiang).
Peer review under responsibility of Chongqing Medical University.

https://doi.org/10.1016/j.gendis.2020.11.009

## Introduction

Osteosarcoma (OS) is the most common primary malignant bone tumour in children and adolescents, accounting for approximately 20% of primary bone cancers.[1,2] OS is prone to occur in the metaphysis of the long bone and is characterized by a high degree of malignancy and metastasis and poor prognosis.[3] It has been reported that approximately 15%—20% of OS patients have distant metastases at the initial diagnosis.[4] Studies have shown that lung metastasis is one of the main causes of death in OS,[5] and the 5-year survival rate of OS with distant metastasis is significantly lower than that without metastasis (20% *vs.* 70%).[6] Therefore, studying the molecular mechanism of OS metastasis will help identify new therapeutic targets and improve prognosis.

Mevalonate is synthesized from 3-hydroxy-3-methylglutaryl coenzyme A (HMG-CoA) by HMG-CoA reductase (HMGCR).[7] Many studies have shown that the mevalonate pathway is upregulated in several cancers, such as breast, hepatic and pancreatic cancers.[8] Brindisi M et al. found that cholesterol and mevalonate were involved in breast cancer progression and drug resistance through the ERR$\alpha$ pathway.[9] The metastasis and chemoresistance of CD133-positive pancreatic cancer cells depend on the activation of the mevalonate pathway.[10] At present, it has been reported that the inhibition of mevalonate pathways can induce OS cell apoptosis,[11] but few studies have focused on its effect on OS metastasis, and the specific molecular mechanism remains unknown.

YAP1 is a transcriptional coactivator that regulates the activity of a variety of transcription factors and participates in the regulation of biological functions such as tumour cell proliferation, migration and invasion.[12] It has been found that inhibition of the mevalonate pathway by simvastatin can inhibit the proliferation and metastasis of breast cancer cells by suppressing YAP1 activity.[13] Although studies have shown that YAP1 is highly expressed in sarcoma tissues and closely related to the stage of the tumour and the prognosis of patients,[14] few studies have explored the relationship between YAP1 and OS metastasis.

In this study, we intended to investigate the effect of the mevalonate pathway on OS metastasis and its molecular mechanism, demonstrating that the mevalonate pathway modulates the metastasis of OS by regulating YAP1 activity via RhoA. Our findings suggest that suppressing the mevalonate pathway may be a potential strategy for the treatment of OS metastasis.

## Materials and methods

### Cell lines and reagents

The human OS cell lines 143B, Saos-2, and MG63 and the osteoblasts cell line hFOB1.19 were purchased from the Shanghai Institute of Biochemistry and Cell Biology, Chinese Academy of Sciences (Shanghai, China), and cultured in DMEM (Gibco, USA) supplemented with 10% FBS (HyClone, USA) and 1% penicillin-streptomycin (HyClone) at 37 °C in 5% $CO_2$. Simvastatin (Sigma—Aldrich, USA, S6196) was activated prior to the experiments by alkaline hydrolysis of the lactone moiety according to the manufacturer's protocol and diluted with serum-free culture medium to various concentrations (0, 1, 2, 4, 8, 16, 32 μM). DL-mevalonolactone (Sigma—Aldrich, M4667) and the Rho inhibitor C3 transferase (Cytoskeleton, USA, CT03) were used to treat cells at concentrations of 250 μM and 3 μg/ml, respectively.

### CCK-8 assay for analysis of cell viability

Cell viability was evaluated using the Cell Counting Kit-8 (CCK-8) assay (Boster, China). Cells were plated into 96-well plates at a concentration of $5 \times 10^3$ cells/well in a medium containing 10% FBS and were cultured for 24 h. Then, the cells were treated with different concentrations of simvastatin for 24 h. Ten microlitres of CCK-8 solution was added to each well, and the cells were incubated for another 1—2 h at 37 °C in the dark. A microplate reader was used to detect the absorbance at 450 nm. Cell viability was calculated using the following equation: cell viability (%) = average OD in the study group/average OD in the control group × 100%.

### Real-time PCR

Total RNA was extracted from cells using TRIzol reagent (TaKaRa, Japan) and then reverse transcribed using the PrimeScript RT Reagent Kit (TaKaRa). Real-time PCR was performed with a SYBR PrimeScript RT-PCR Kit (TaKaRa) according to the manufacturer's instructions. Real-time PCR cycles were as follows: initiation with a 3-min denaturation at 95 °C followed by 40 amplification cycles with 15 s of denaturation at 95 °C, 30 s of annealing at 60 °C and 30 s of extension at 72 °C. Gene expression levels were normalized with the *GAPDH* housekeeping gene. The examined genes and their PCR primers are listed in Supplemental materials: Table S1.

### Membrane protein extraction

Because the active form of RhoA binds to the membrane and the inactive form is located in the cytoplasm, the content of activated RhoA was detected by cell membrane separation. The membrane and cytosol were isolated by using a Membrane Protein Extraction Kit (Sangon Biotech, China) according to the manufacturer's instructions. The extracted membrane protein was used for western blot detection.

### Western blot

After cells in the logarithmic growth phase were treated according to their group, the cells were collected, and total protein was extracted using RIPA cell lysate (Beyotime, China). The protein concentrations were determined using the BCA assay method (Beyotime), and 30 μg total protein per sample was used after boiling and denaturation.

Following 7.5% or 12.5% SDS-PAGE (EpiZyme, China), proteins were transferred onto PVDF membranes. The PVDF membranes were incubated with QuickBlock™ Blocking Buffer (Beyotime) at room temperature for 15 min, and the corresponding primary antibodies were then added and incubated at 4 °C overnight: anti-E-Cadherin (1:1000; CST, USA, 3195), anti-N-Cadherin (1:1000; CST, 13116), anti-Vimentin (1:1000; CST, 5741), anti-MMP2 (1:1000; CST, 40994), anti-HMGCR (1:1000; CST, 36877), anti-RhoA (1:1000; CST, 2117), anti-YAP1 (1:1000; CST, 14074), anti-p-YAP1 (1:1000; CST, 13008) and anti-GAPDH (1:3000; Bioss, China, bs-0755R). After the membranes were rewarmed at room temperature for 30 min, they were rinsed four times with TBST [TBS (Solarbio, China) + 0.05% Tween-20 (Solarbio)], and a horseradish peroxidase-labelled secondary antibody (1:10000; Bioss, bs-0295G) was added to the blots and incubated for 1.5 h at room temperature. Following washing with TBST, the images were analysed by ECL chemiluminescence (Millipore, USA) using VILBER Fusion FX7 software.

## Immunofluorescence

Cells were seeded in laser confocal plates (NEST, China) at a density of $3 \times 10^4$ cells/plate and treated according to their groups for 24 h. Subsequently, the cells were washed with PBS, fixed in 4% paraformaldehyde (Beyotime) for 20 min, and permeabilized in PBS with 0.1% Triton X-100 (Sigma—Aldrich) for 15 min. The cells were then incubated in goat serum (Beyotime) for 30 min at 37 °C and treated with anti-YAP1 antibody (1:100; CST, 14074) and incubated at 4 °C overnight. The next day, a secondary antibody, FITC-conjugated goat anti-rabbit IgG (1:1000; CST, 4412), was applied for 1 h at 37 °C, and then, nuclei were counterstained with DAPI (Bioss, C02-04002). Laser confocal plates were viewed under a fluorescence microscope (Axio Observer A1; Carl Zeiss AG, Oberkochen, Germany).

## Transfection

YAP1 and RhoA overexpression lentiviruses were designed, synthesized and sequenced by Hanbio Biotechnology (Shanghai, China). The amplified primer sequences are listed in Supplemental materials: Table S2.

Short hairpin RNA (shRNA) targeting YAP1 (shYAP1) and its control (shNT) were purchased from Hanbio Biotechnology (Shanghai, China). The shRNA target sequences are listed in Supplemental materials: Table S3.

The 143B cells were infected with the lentivirus vectors according to the manufacturer's instructions. The knockdown or overexpression efficacy was verified using real-time PCR and western blot analysis.

## Wound healing assay

Cells were seeded into 6-well plates ($2 \times 10^6$ cells/well). After 70% confluence was reached, a 10-μl pipette tip was used to make a scratch. The wells were washed with PBS to remove the floating cells, and 2 ml of serum-free culture medium was added. Then, the plates were placed at 37 °C in 5% $CO_2$. After 24 h, cell migration was observed under an inverted light microscope, and the scratch width was measured by ImageJ 2.1.4 (National Institutes of Health).

## Transwell assay

For the Transwell migration or invasion assays, 143B cells were resuspended in DMEM without serum and seeded into the upper chamber of 8-μm Transwell chambers (Corning, USA) ($3 \times 10^5$ cells/ml). The invasion assay was performed using chambers precoated with 1:8 diluted Matrigel (Corning, USA), while the migration assay was not. DMEM containing 15% FBS was added to the lower chambers (24-well plate), and the cells were incubated for 16 h for the migration assay and 24 h for the invasion assay. After incubation at 37 °C in a 5% $CO_2$ incubator, the chambers were removed, and the Matrigel and the cells in the upper chambers were carefully wiped away with a cotton swab. The migrating or invading cells that had passed through the membrane were fixed with 4% paraformaldehyde (Beyotime) for 15 min, stained with 0.1% crystal violet (Beyotime) for 15 min and counted using an Olympus upright light microscope.

## Immunohistochemistry (IHC)

IHC was performed using an IHC kit (Boster). Samples were deparaffinized through a series of xylene baths, antigen was retrieved by steam treatment in 10 mM citrate buffer, and the samples were blocked with 3% hydrogen peroxide for 15 min at 37 °C, preincubated with blocking serum solution for 30 min at 37 °C and then incubated at 4 °C with the primary antibodies overnight. The primary antibodies were as follows: anti-YAP1 (1:400; CST, 14074) and anti-RhoA (1:400; CST, 2117). Subsequently, the secondary antibodies were applied, and the nuclei were counterstained with haematoxylin. The slides were then examined from nonoverlapping cells using an Olympus BX50 light microscope.

## *In vivo* lung metastasis model

Ten 4-week-old female nude mice were randomly divided into 2 groups: the control group and the simvastatin group. Five mice in the simvastatin group were injected intraperitoneally daily with simvastatin (5 mg/kg) for 9 days, and five mice in the control group received PBS solution. Then, 143B cells ($5 \times 10^6$ cells) were injected into the tail vein of nude mice in a volume of 100 μl. After injection of 143B cells, simvastatin was continually administered until 21 days.

The mice were evaluated every three days for weight. The death of the nude mice was recorded to calculate the lifetime at 39 days. All mice were sacrificed at 39 days. All lungs were resected and fixed in 4% paraformaldehyde (Beyotime). The fixed lungs were embedded in paraffin, sectioned, and stained with H&E (Beyotime). RhoA and YAP1 expression levels in lung metastatic nodules were quantified by IHC. A light microscope was used to determine whether there was a metastatic nodule and count the number of lung metastatic nodules.

### Statistical analysis

Quantitative data are presented as the mean ± SD and were compared using Student's *t*-test or ANOVA. Categorical data were analysed using the Chi-squared test or Fisher's exact test. Survival analysis was carried out using the Kaplan–Meier method with the log-rank test. $P < 0.05$ was considered statistically significant. All analyses were performed using SPSS 20.0 software (Chicago, IL, USA) or GraphPad Prism 7.00 (San Diego, CA, USA).

## Results

### Epithelial-mesenchymal transition (EMT) and the mevalonate pathway are significantly activated in OS cells

Western blot analysis showed that the expression of the N-Cadherin, Vimentin and MMP2 proteins in OS cells (143B, Saos-2 and MG63) was significantly higher than that in osteoblasts, while the expression of E-cadherin was significantly lower (Fig. 1A,B). This result indicated that the EMT process of OS cells was significantly enhanced. Moreover, real-time PCR and western blot analysis showed that the HMGCR mRNA and protein levels in OS cells (143B, Saos-2 and MG63) were also significantly upregulated compared with those in osteoblasts (Fig. 1C–E). Thus, the mevalonate pathway may regulate the EMT process of OS cells.

### The mevalonate pathway promotes the motility of 143B cells

CCK-8 assays showed that suppressing the mevalonate pathway by simvastatin inhibited the viability of 143B cells in a time- and dose-dependent manner, and the 50% inhibitory concentrations ($IC_{50}$) at 24 h and 48 h were 24 μM and 16 μM, respectively (Fig. 2A). Thus, 2 μM simvastatin treatment for 24 h did not significantly inhibit the viability of 143B cells. The wound healing assay showed that simvastatin could inhibit the migration of 143B cells, and mevalonate supplementation reversed this inhibition (Fig. 2B,C). *In vitro* Transwell assays further confirmed the above effects of simvastatin and mevalonate (Fig. 2D–F). In addition, western blot analysis showed that simvastatin inhibited the EMT process of 143B cells, which was reflected by decreased N-Cadherin, Vimentin and MMP2 and increased E-cadherin, whereas mevalonate abolished this inhibitory effect (Fig. 2G,H). These results showed that the mevalonate pathway promotes the motility of 143B cells.

### YAP1 activity is significantly upregulated in OS cells

First, we detected the YAP1 mRNA and protein levels in different cells and found that YAP1 expression in OS cells (143B, Saos-2 and MG63) was higher than that in osteoblasts (hFOB1.19) (Fig. 3A–C). YAP1 expression in the 143B cells was the highest, so we chose 143B cells for the following experiment. Then, we used immunofluorescence staining to identify the cellular localization of YAP1. The results showed that YAP1 in 143B cells was mainly located in the nucleus, while in hFOB1.19 cells, YAP1 was mainly located in the cytoplasm (Fig. 3D,E). These above results suggested that YAP1 activity is significantly upregulated in OS cells and thus may be involved in the biological function of OS cells.

### YAP1 modulates the motility of 143B cells

To further assess the functional role of YAP1 in OS cells, we first used shRNA to knock down YAP1 in 143B cells and verified

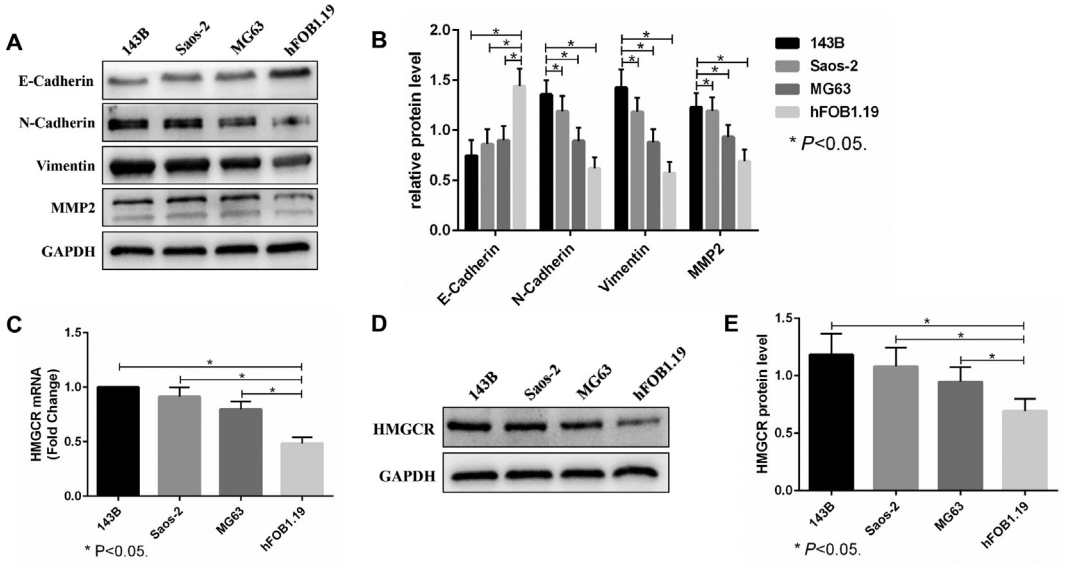


**Figure 1** Epithelial-mesenchymal transition (EMT) and the mevalonate pathway are significantly activated in OS cells. **(A, B)**. The expression of E-Cadherin, N-Cadherin, Vimentin and MMP2 in OS cells (143B, Saos-2 and MG63) and normal osteoblasts (hFOB1.19) was evaluated by western blots. GAPDH was used as a reference. **(C–E)**. The HMGCR mRNA and protein levels of OS cells and normal osteoblasts were analysed by real-time PCR (C) and western blots (D, E). GAPDH was used as a reference. The bars show the mean ± SD of three independent experiments.

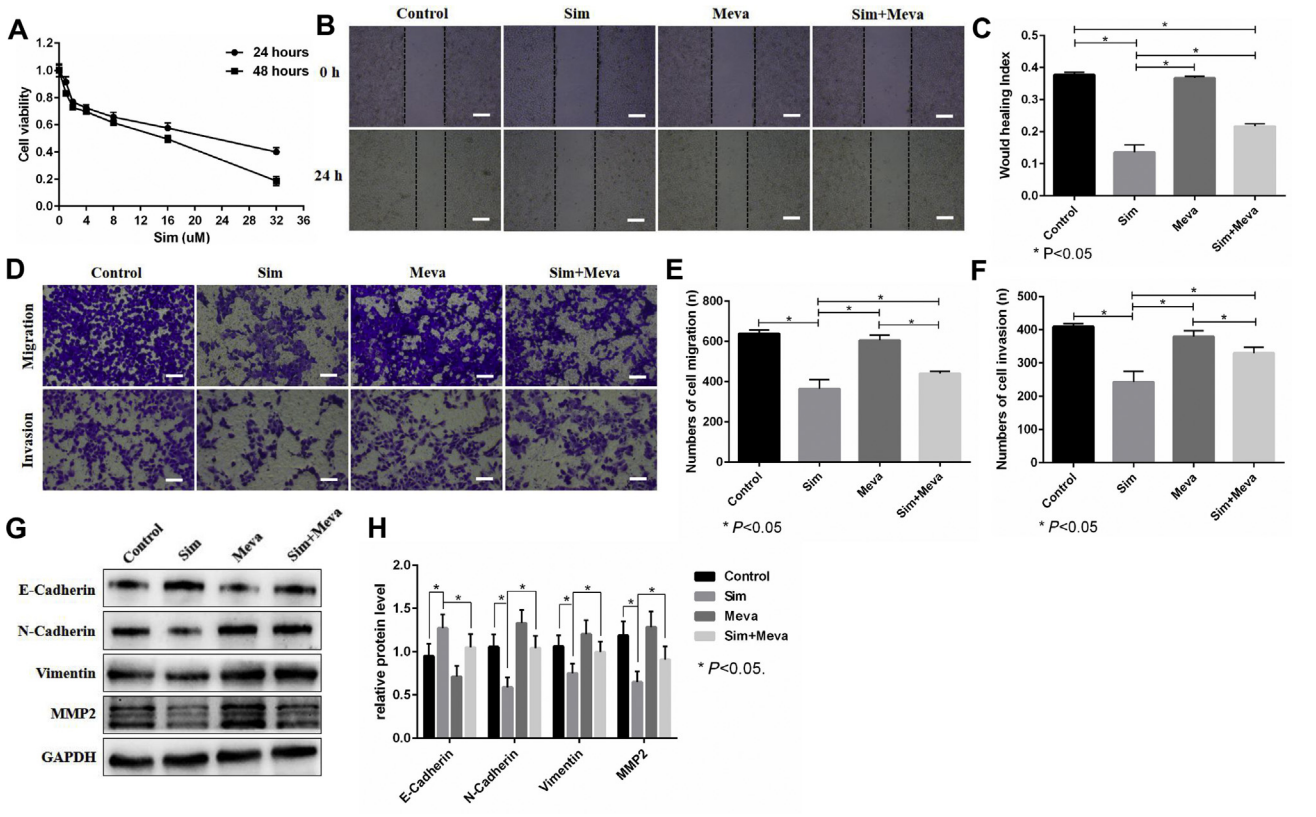


**Figure 2** The mevalonate pathway promotes the motility of 143B cells. **(A)**. The effect of simvastatin (Sim) on 143B cell viability was detected through CCK-8 assays. **(B—F)**. First, 143B cells were incubated with or without 250 μM mevalonate (Meva) for 6 h before treatment with DMSO or 2 μM Sim for 24 h and then used for wound healing assays (24 h) (B, C) and Transwell migration (16 h) and invasion (24 h) assays (D—F). Scale bars: 200 μm. **(G, H)**. The expression of E-Cadherin, N-Cadherin, Vimentin and MMP2 was evaluated by western blots. GAPDH was used as a reference. The bars show the mean ± SD of three independent experiments.

the knockdown efficacy by real-time PCR and western blots (Fig. 4A—C). The knockdown efficacy of shYAP1-2 was the most obvious, so we chose shYAP1-2 (recorded as shYAP1) for the following experiment. Wound healing assays showed that knockdown of YAP1 inhibited the migration of 143B cells (Fig. 4D,E). Moreover, Transwell assays revealed that knockdown of YAP1 suppressed the migration and invasion of 143B cells (Fig. 4F—H). Moreover, western blot analysis showed that knockdown of YAP1 inhibited the EMT process of 143B cells, which was reflected by the decreased N-Cadherin, Vimentin and MMP2 levels and increased E-cadherin levels (Fig. 4I,J). These results together showed that the upregulated YAP1 was positively correlated with the migration and invasion of 143B cells.

## The mevalonate pathway promotes the motility of 143b cells by regulating YAP1 activity

YAP1 activity is known to depend on its cellular localization, which, in turn, is determined by its phosphorylation status. Western blot analysis showed that suppressing the mevalonate pathway by simvastatin induced an increase in YAP1 phosphorylation in 143B cells, and this effect was abolished by adding mevalonate (Fig. 5A,B), which suggested that the mevalonate pathway modulates YAP1 activity by regulating its phosphorylation. We then examined the localization of YAP1 in 143B cells treated with simvastatin. Consistent with the increased YAP1 phosphorylation level, simvastatin induced YAP1 translocation from the nucleus to the cytoplasm, as visualized by immunofluorescence staining, whereas adding mevalonate prevented this translocation (Fig. 5C,D). To further assess the functional role of YAP1 in the process of the mevalonate pathway regulating the migration and invasion of OS cells, we first used a lentiviral vector to upregulate YAP1 in 143B cells and verify the overexpression efficacy by real-time PCR and western blots (Fig. 5E—G). Wound healing assays showed that the overexpression of YAP1 reversed the inhibition of migration of 143B cells caused by simvastatin (Fig. 5H,I). *In vitro* Transwell assays further confirmed the above effects of YAP1 overexpression (Fig. 5J-L). In addition, western blot analysis showed that the overexpression of YAP1 abolished the inhibitory effect of simvastatin on EMT, which was reflected by increased N-Cadherin, Vimentin and MMP2 and decreased E-cadherin (Fig. 5M,N). Taken together, our results revealed that the mevalonate pathway promotes the motility of 143B cells by regulating YAP1 activity.

## The mevalonate pathway regulates YAP1 activity via RhoA activation

The active form of RhoA is located in the cell membrane, while the inactive form is located in the cytoplasm. After cell membrane separation, western blot analysis showed

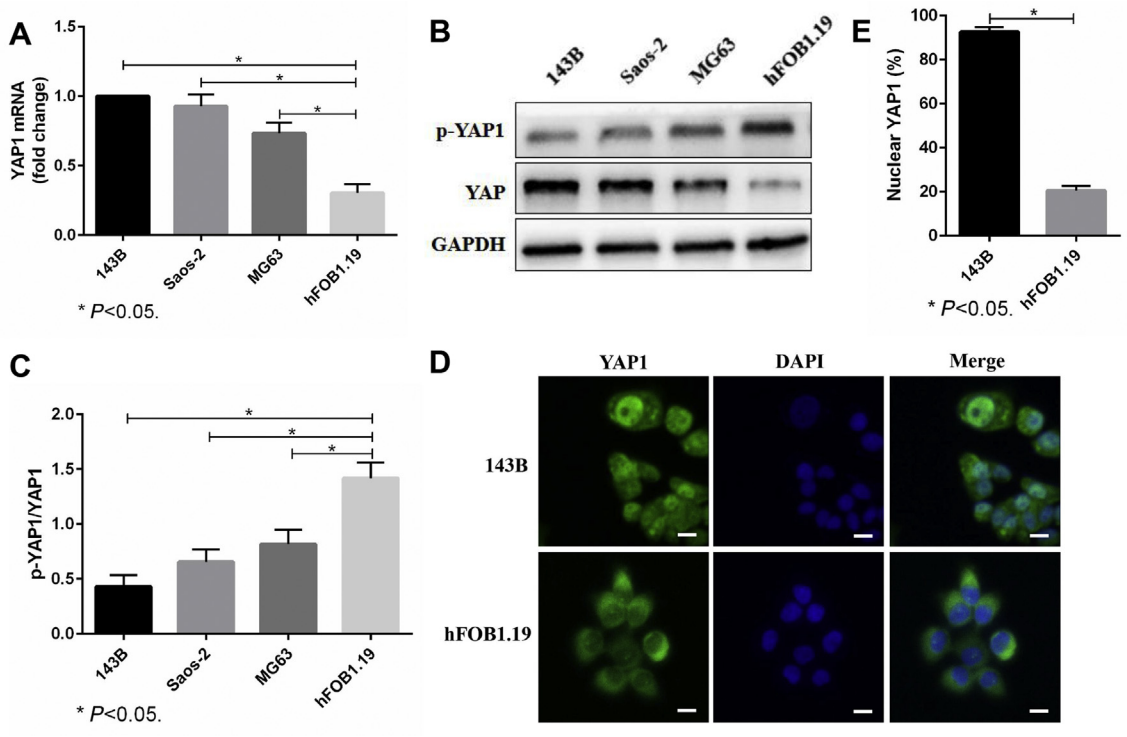


**Figure 3** YAP1 activity is significantly upregulated in OS cells. **(A—C)**. The YAP1 mRNA and p-YAP1/YAP1 protein levels of OS cells (143B, Saos-2 and MG63) and normal osteoblasts (hFOB1.19) were evaluated through real-time PCR (A) and western blots (B, C). GAPDH was used as a reference. **(D, E)**. The cellular localization of YAP1 in 143B cells and hFOB1.19 cells was detected by immunofluorescence staining. Cells were fixed and stained with YAP1 antibody (green) and DAPI (blue). Scale bars: 50 μm. The bars show the mean ± SD of three independent experiments.

that simvastatin could significantly inhibit the cell membrane RhoA, while mevalonate supplementation could promote the cell membrane localization of RhoA (Fig. 6A, B). To further explore the relationship between RhoA activation and YAP1 activity, we first treated 143B cells with C3 transferase (a RhoA inhibitor) and found that it significantly increased YAP1 phosphorylation (Fig. 6C,D). Moreover, we used a lentiviral vector to upregulate RhoA in 143B cells and verified the overexpression efficacy by real-time PCR and western blots (Fig. 6E—G). Western blot analysis showed that the upregulation of RhoA abolished the increase in YAP1 phosphorylation induced by simvastatin (Fig. 6H,I). Consistent with the YAP1 phosphorylation, immunofluorescence staining revealed that the overexpression of RhoA prevented YAP1 translocation from the nucleus to the cytoplasm caused by simvastatin (Fig. 6J,K). All of the above results suggested that the mevalonate pathway regulates YAP1 activity via RhoA activation.

## Suppressing the mevalonate pathway inhibits 143B cell-induced lung metastasis *in vivo*

To further investigate whether suppressing the mevalonate pathway inhibits OS-induced lung metastasis, we established a lung metastasis model *in vivo* by injecting stable 143B cells into the tail vein of nude mice. We found that suppressing the mevalonate pathway by simvastatin notably reduced the ability of 143B OS cells to induce lung metastases, as reflected by the decreased incidence and number of metastatic nodules and the increased survival time of the mice (Fig. 7A—D). Also, RhoA and YAP1 were found with high expression in lung metastatic nodules (Fig. 7E). However, simvastatin had no significant influence on the body weight of the nude mice (Fig. 7F). These results, together with our *in vitro* findings, highlighted the functional role of the mevalonate pathway in the regulation of OS-induced lung metastasis.

## Discussion

Previous studies have found that the mevalonate pathway is highly activated in a variety of tumours, as reflected by upregulated HMGCR.[15—17] The activated mevalonate pathway is positively correlated with tumour cell proliferation and metastasis, such as that in gastric, breast and prostate cancer.[8] In this study, we also found upregulated HMGCR expression in OS cells compared to normal osteoblasts. In addition, we detected high EMT activity in OS cells. Therefore, we speculate that the mevalonate pathway may regulate OS metastasis.

A growing number of studies suggest that suppressing the mevalonate pathway by statins inhibits the proliferation, migration and invasion of cancer cells.[18,19] Sorrentino G et al. found that suppression of HMGCR by statins inhibits the proliferation and self-renewal of breast cancer cells.[20] Specific blockade of the mevalonate pathway with lipophilic statins led to apoptosis and substantial growth

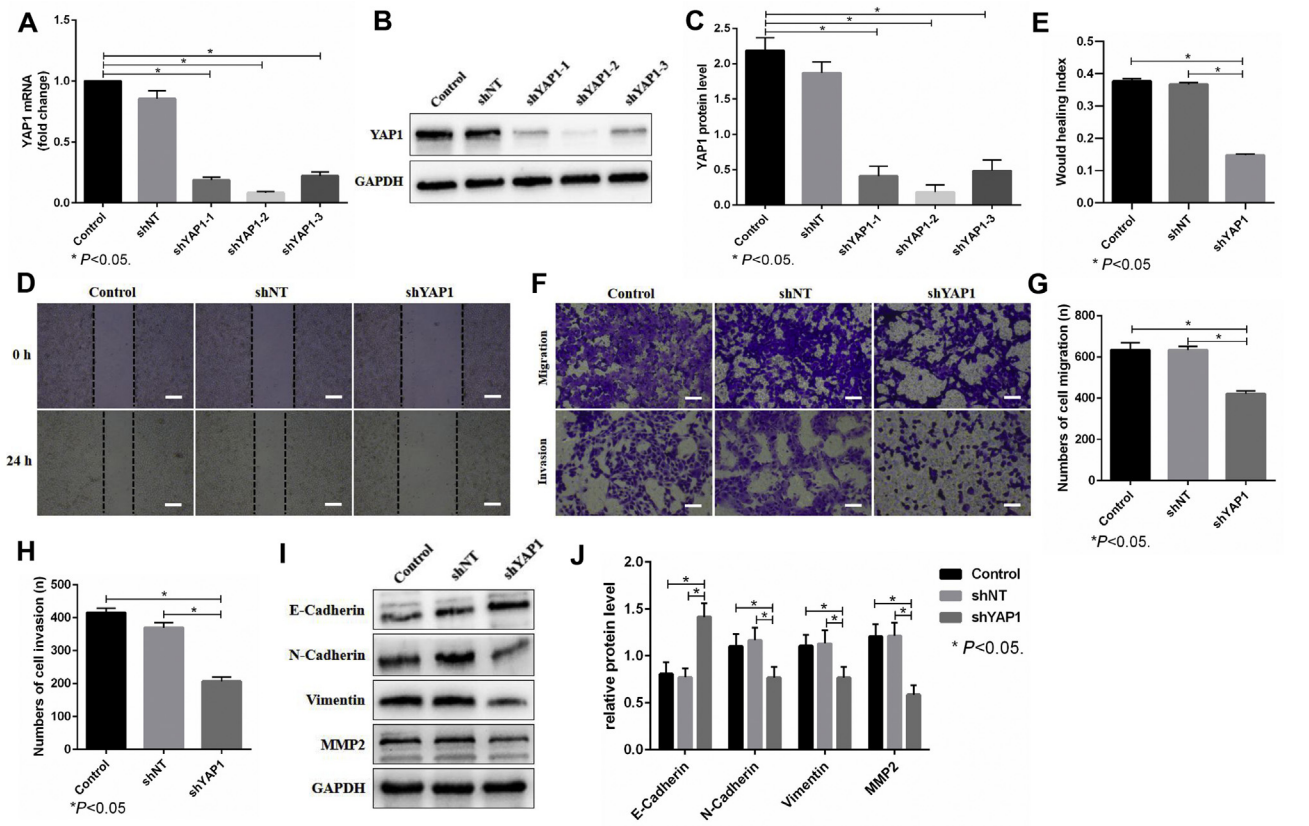


**Figure 4** YAP1 modulates the motility of 143B cells. **(A—C)**. The 143B cells were transfected with lentiviral vector targeting YAP1 and its control (shNT). The knockdown efficacy of YAP1 was evaluated through real-time PCR (A) and western blots (B, C). GAPDH was used as a reference. shYAP1-1 (recorded as shYAP1) was chosen for the following experiment. **(D, E)**. The migration of 143B cells with YAP1 knockdown was detected by a wound healing assay (24 h). Scale bars: 200 μm. **(F—H)**. The migration (16 h) and invasion (24 h) of 143B cells with YAP1 knockdown was detected by Transwell assay. Scale bars: 200 μm. **(I, J)**. The expression of E-Cadherin, N-Cadherin, Vimentin and MMP2 was evaluated by western blots. GAPDH was used as a reference. The bars show the mean ± SD of three independent experiments.

inhibition of HER2$^+$ breast cancer.[21] Consistent with these results, in this study, we also found that simvastatin inhibited the migration and invasion of 143B cells, and supplementation with mevalonate reversed this inhibition.

In this study, we found overexpression and high activity of YAP1 in OS cells compared to osteoblasts. These data suggest that YAP1 may play a critical role in the biological function of OS. Increasing evidence has shown the importance of YAP in the pathogenesis of different tumours.[22] For example, YAP was found to be upregulated in prostate, breast and ovarian tumours.[23—25] YAP overexpression promotes the growth of subcutaneous xenografts of cervical squamous cell carcinomas.[26] Inhibition of YAP by verteporfin could effectively inhibit bladder cancer cell growth and invasion.[27] Additionally, knockdown of YAP strongly reduced the rates of migration and invasion of prostate cancer cells.[28] However, the functions of YAP in OS cells are poorly understood. The YAP level was found to be upregulated in approximately 80% of OS tissues compared with normal bone tissues.[29] YAP knockdown impaired the growth of primary mouse OS cell lines.[30] To the best of our knowledge, few studies have explored the relationship between YAP and OS metastasis. In this study, we used shRNA to knock down YAP1 and found that knockdown of YAP1 significantly inhibited the migration and invasion of 143B cells. The above findings suggest that YAP1 plays an important role in OS metastasis.

YAP activity depends on its cellular localization, which, in turn, is determined by its phosphorylation status. Phosphorylation of YAP induces translocation of YAP from the nucleus to the cytoplasm, thus reducing the transcriptional activity of TEAD. Studies have concluded that the mevalonate pathway regulates the cellular location and phosphorylation status of YAP.[31—33] Liu Q et al. concluded that simvastatin could inhibit proliferation, migration and invasion and promote apoptosis in gastric cancer cells by suppressing the activity of YAP.[34] Wang Z et al. also found that simvastatin significantly inhibits the migration and invasion of breast cancer cells by regulating the YAP cellular location and phosphorylation status.[35] In this study, we also explored the influence of the mevalonate pathway on YAP1 activity. The results demonstrated that simvastatin increased the phosphorylation level of YAP1 and induced translocation of YAP1 from the nucleus to the cytoplasm, whereas adding mevalonate prevented the above process. These results strongly indicate that the mevalonate pathway modulates

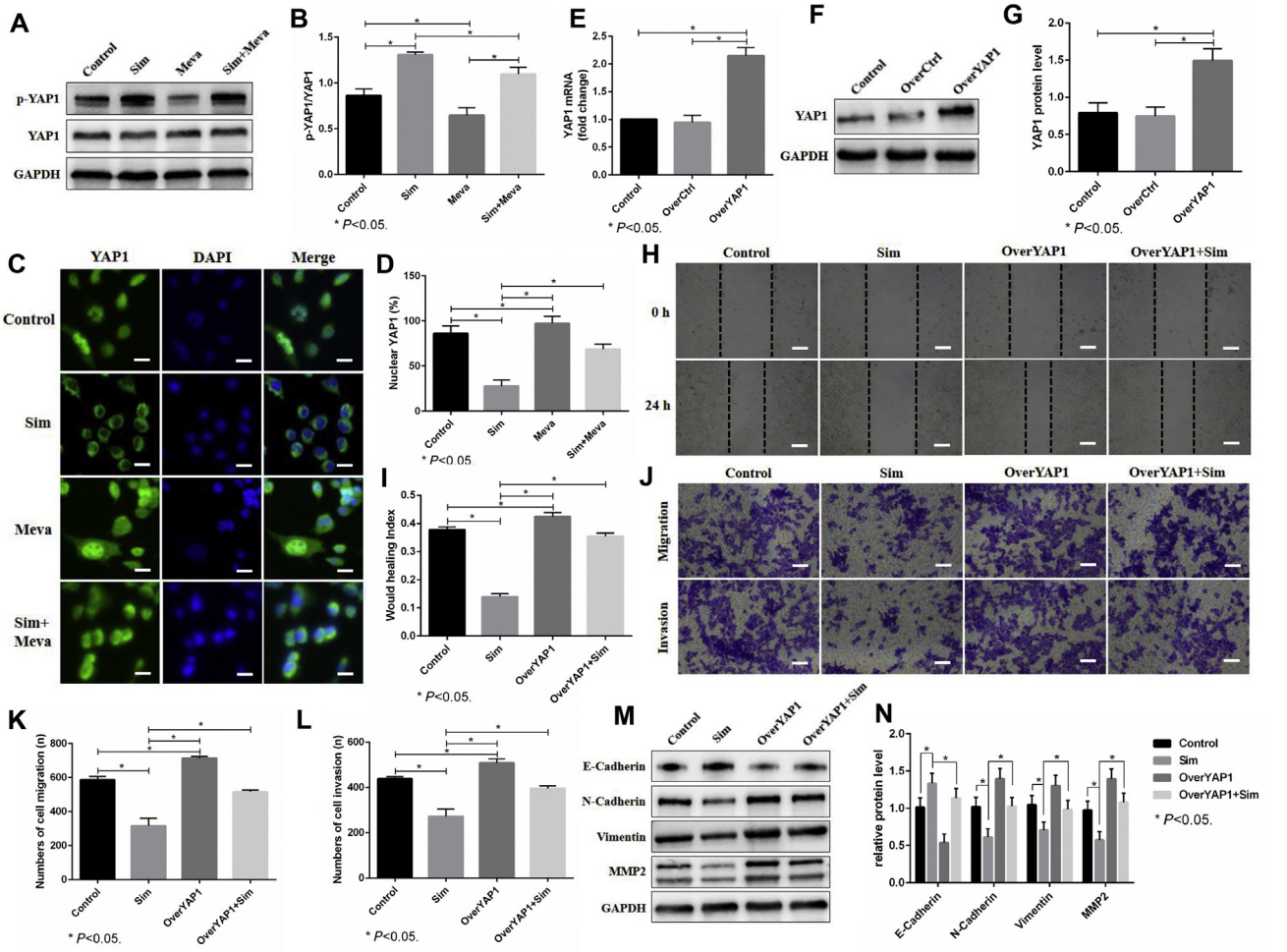


**Figure 5** The mevalonate pathway promotes the motility of 143b cells by regulating YAP1 activity. **(A, B)**. First, 143B cells were treated with or without 250 μM mevalonate (Meva) for 6 h before incubation with DMSO or 2 μM simvastatin (Sim) for 24 h. The expression of p-YAP1 and YAP1 was evaluated by western blots. **(C, D)**. The cellular localization of YAP1 in 143B cells was detected by immunofluorescence staining. The cells were fixed and stained with YAP1 antibody (green) and DAPI (blue). Scale bars: 50 μm. **(E—G)**. The 143B cells were transfected with lentiviral vector with YAP1 overexpression (OverYAP1) and its control (OverCtrl). The efficacy of YAP1 overexpression was evaluated through real-time PCR (E) and western blots **(F, G)**. GAPDH was used as a reference. **(H—L)**. The motility of 143B cells was detected by wound healing assays **(H, I)** and Transwell assays (J—L). Scale bars: 200 μm. Sim treatment (2 μM for 24 h) inhibited the motility of 143B cells, while overexpression of YAP reversed this inhibition. **(M, N)**. The expression of E-Cadherin, N-Cadherin, Vimentin and MMP2 was evaluated by western blots. GAPDH was used as a reference. The bars show the mean ± SD of three independent experiments.

the migration and invasion of 143B cells by regulating YAP1 phosphorylation and cellular localization.

The mevalonate pathway has been shown to regulate numerous pathways, including epigenetic pathways, Ras and Rho.[7] Karlic H et al. concluded that inhibition of the mevalonate pathway affects epigenetic regulation in many cancer cell lines, as reflected by aberrant stimulation of DNA methyltransferase (DNMT1) and changes in histone deacetylases (HDACs) and microRNAs.[36] Prenylation of Ras and Rho is crucial for cancer progression and metastasis.[37] Farnesylation of Ras GTPase, which is regulated by the mevalonate pathway, has been shown to play crucial roles in Ras activation and tumour progression.[8] Inhibition of farnesyl diphosphate synthase (FDPS) suppresses cell proliferation with decreased Ras farnesylation, and this inhibition can be partially rescued by supplementation with farnesyl pyrophosphate (FPP).[38,39] Similar to Ras, the production of geranylgeranyl pyrophosphate (GGPP) through the mevalonate pathway is required for Rho genarylgenarylation and tumour progression.[8,20] Blocking the mevalonate pathway inhibits viable cell proliferation and induces apoptosis, which is nullified by supplementation with GGPP.[20,40] Although the mevalonate pathway has been proven to modulate the activities of oncogenic proteins by regulating their prenylation, the specific mechanism of its regulation of YAP is still unclear. It was reported that the nuclear localization and activity of YAP were regulated through the mevalonate pathway via Rho activity.[20,35] Therefore, in this study, we investigated the role of Rho in the regulation of YAP by the mevalonate pathway.

The Rho family of GTPases is a well-known regulator of cell migration and invasion and has been implicated in the

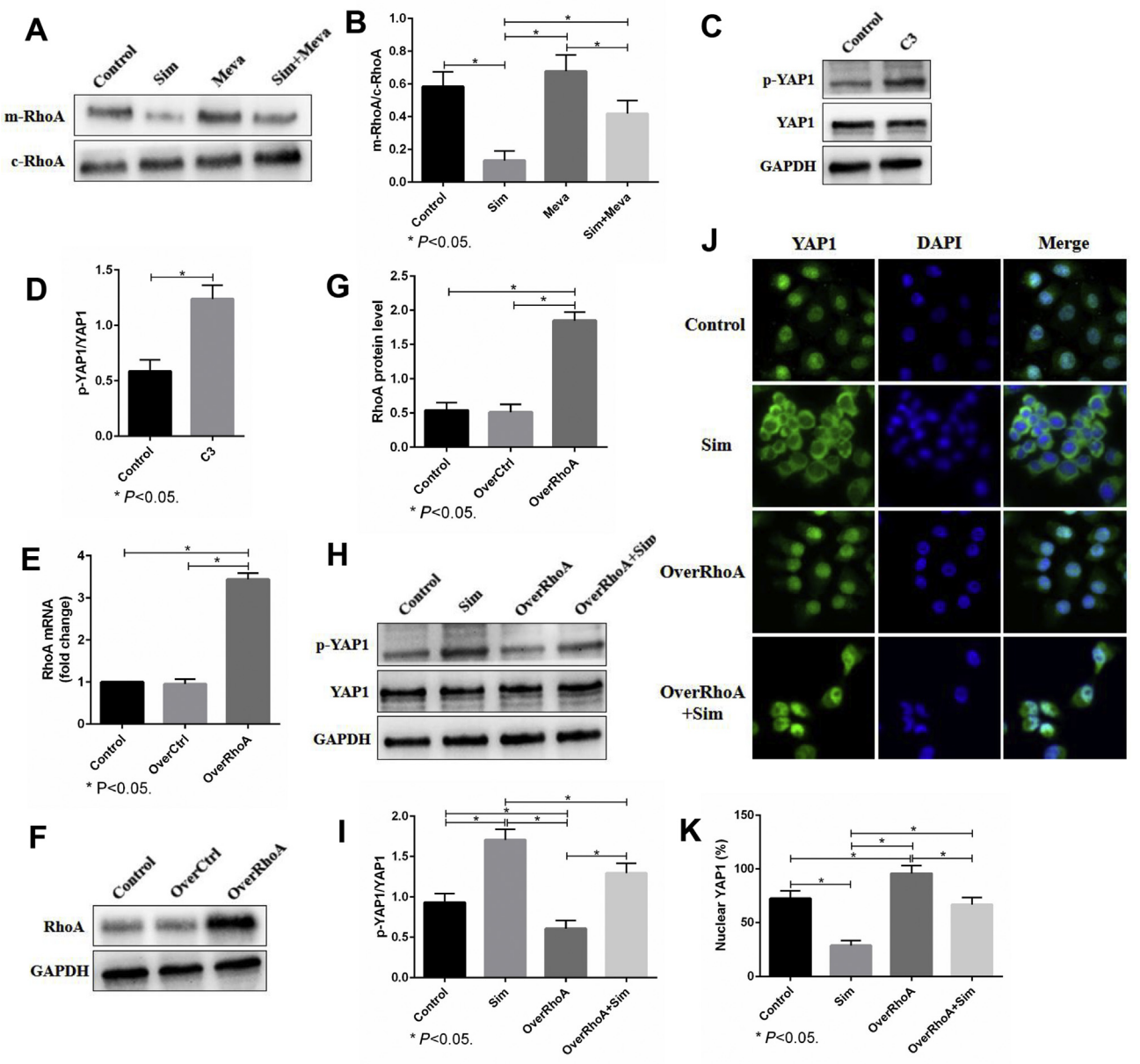


**Figure 6** The mevalonate pathway regulates YAP1 activity via RhoA activation. **(A, B)**. After cell membrane separation, membrane RhoA (mRhoA) and cytoplasm RhoA (cRhoA) were evaluated by western blots. **(C, D)**. First, 143B cells were treated with or without 3 μg/ml C3 transferase (C3) for 24 h. The expression of p-YAP1 and YAP1 was evaluated by western blots. **(E—G)**. A lentiviral vector was used to upregulate RhoA in 143B cells, and the overexpression efficacy was verified by real-time PCR (E) and western blots **(F, G)**. GAPDH was used as a reference. **(H, I)**. The cellular localization of YAP1 in 143B cells was detected by immunofluorescence staining. The cells were fixed and stained with YAP1 antibody (green) and DAPI (blue). Scale bars: 50 μm. **(J, K)**. The expression of E-Cadherin, N-Cadherin, Vimentin and MMP2 was evaluated by western blots. GAPDH was used as a reference. The bars show the mean ± SD of three independent experiments.

process of tumour metastasis.[41] The RhoA signalling pathway is strongly correlated with the ability of tumour cells to invade and successfully establish metastases.[42] Zaoui K et al. found that the Ran protein induced invasion of ovarian cancer cells by promoting and stabilizing the cell membrane localization of RhoA.[43] Kim YN et al. found that resveratrol suppressed breast cancer cell invasion by inhibiting YAP signalling through inactivation of RhoA.[44] In this study, we first found that suppressing the mevalonate pathway could significantly inhibit the cell membrane localization of RhoA. Moreover, inhibition of RhoA by C3 transferase increased YAP1 phosphorylation, while RhoA overexpression decreased YAP1 phosphorylation and induced the translocation of YAP1 from the cytoplasm to

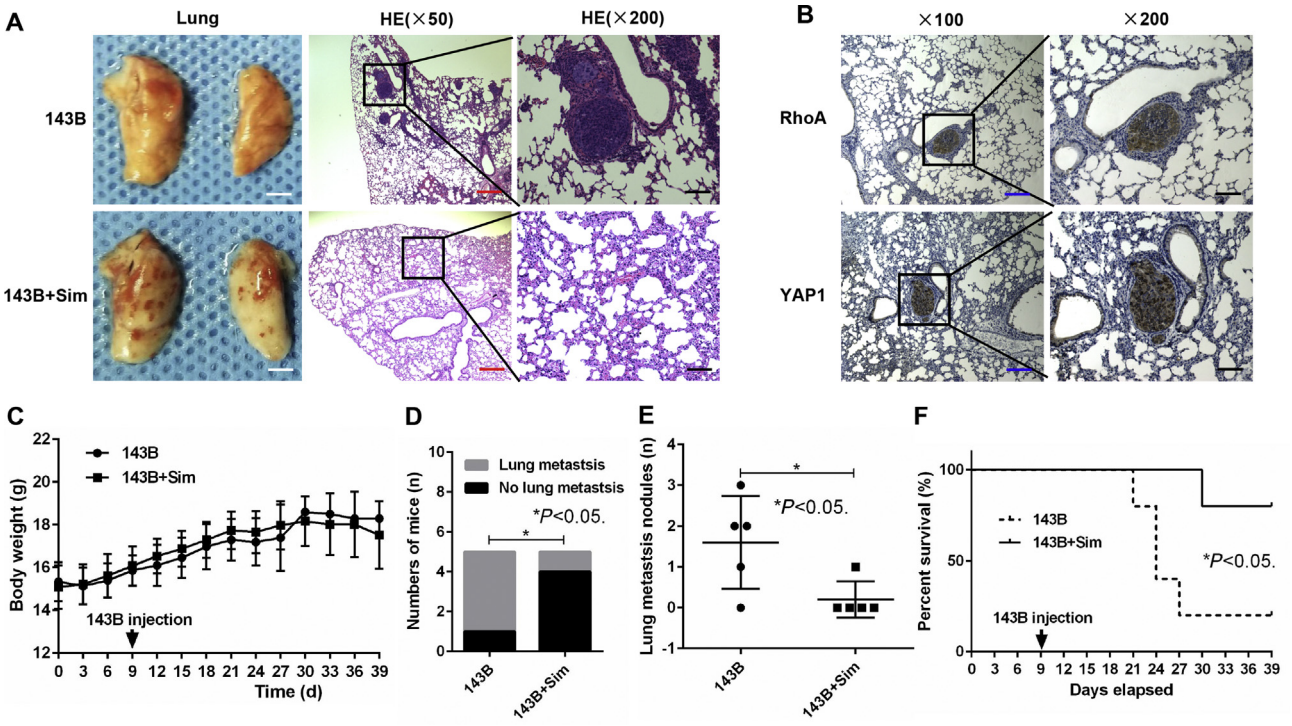


**Figure 7** Suppressing the mevalonate pathway inhibits 143B cell-induced lung metastasis *in vivo*. **(A)** First, 143B cells were injected into the tail vein of nude mice to establish an *in vivo* model of lung metastasis, and then, the mice received simvastatin (143B + Sim) or were left untreated (143B). Representative macroscopic and microscopic images (H&E staining) of the lungs. White scale bars: 400 mm, red scale bars: 200 μm, black scale bars: 50 μm. **(B)** Percentage of mice bearing lung metastases in each group ($n = 5$). **(C)** Numbers of lung metastatic nodules quantified on sections with H&E staining of the lungs. **(D)** Kaplan–Meier overall survival curves of each group ($n = 5$) at 39 days. Significant differences were determined using the log-rank test. **(E)** RhoA and YAP1 expression levels in lung metastatic nodules was quantified by IHC. Blue scale bars: 100 μm, black scale bars: 50 μm. **(F)** Body weight of mice in each group ($n = 5$).

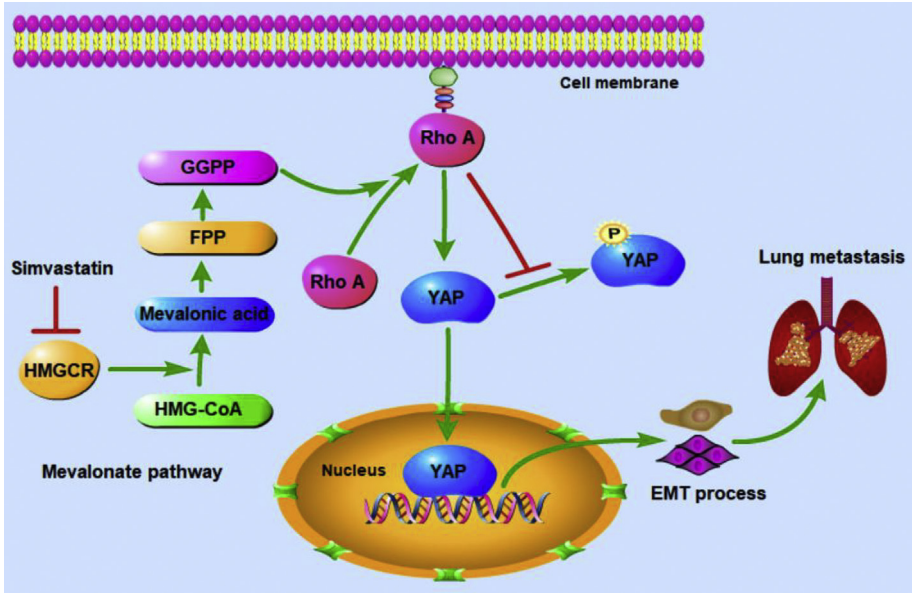


**Figure 8** The possible mode of action of the mevalonate pathway in OS metastasis. The activated mevalonate pathway promotes the prenylation and activities of RhoA, leading to its translocation to the plasma membrane and activation of YAP1. Nuclear translocated YAP1 promotes transcription of downstream target genes and induces OS cell EMT and lung metastasis.

the nucleus. These results strongly indicate that the mevalonate pathway modulates YAP1 phosphorylation and localization by regulating RhoA activity.

We also further investigated whether suppressing the mevalonate pathway inhibits OS-induced lung metastasis *in vivo*. It was demonstrated that simvastatin notably reduced the ability of 143B cells to induce lung metastases, as reflected by the decreased incidence and number of metastatic nodules and the increased survival time of the mice. Also, RhoA and YAP1 were found with high expression in lung metastatic nodules. However, simvastatin showed no significant influence on the body weight of nude mice, which may be because the weight loss caused by OS lung metastasis cannot be obviously distinguished from that caused by the lipid-lowering effects of simvastatin. These *in vivo* results are in agreement with our results from cellular investigations and establish the physiological and pathological significance of the mevalonate pathway in regulating OS metastasis. Therefore, the inhibition of the mevalonate pathway is a promising therapeutic strategy in OS metastasis. The possible mode of action of the mevalonate pathway in OS metastasis is shown in Figure 8.

In conclusion, our results demonstrated that suppressing the mevalonate pathway inhibits OS metastasis by inhibiting YAP1 activity through inactivation of RhoA activity. These findings suggest that inhibition of the mevalonate pathway may be a potential strategy for the treatment of OS.

## Conflict of interests

The authors have no conflict of interests to declare.

## Funding

This work was supported by the Natural Science Foundation of Chongqing (No.cstc2019jcyj-msxmX0358).

## Appendix A. Supplementary data

Supplementary data to this article can be found online at https://doi.org/10.1016/j.gendis.2020.11.009.

## References

1. Bao B, Zhou Y, Lu W, et al. Incidence and mortality of sarcomas in Shanghai, China, during 2002-2014. *Front Oncol*. 2019;9:662.
2. Kollár A, Rothermundt C, Klenke F, et al. Incidence, mortality, and survival trends of soft tissue and bone sarcoma in Switzerland between 1996 and 2015. *Cancer Epidemiol*. 2019;63:101596.
3. Ferrari A, Dirksen U, Bielack S. Sarcomas of soft tissue and bone. *Prog Tumor Res*. 2016;43:128—141.
4. Zhang C, Guo X, Xu Y, et al. Lung metastases at the initial diagnosis of high-grade osteosarcoma: prevalence, risk factors and prognostic factors. A large population-based cohort study. *Sao Paulo Med J*. 2019;137(5):423—429.
5. Meazza C, Scanagatta P. Metastatic osteosarcoma: a challenging multidisciplinary treatment. *Expert Rev Anticancer Ther*. 2016;16(5):543—556.
6. Kelley LM, Schlegel M, Hecker-Nolting S, et al. Pathological fracture and prognosis of high-grade osteosarcoma of the extremities: an analysis of 2,847 consecutive Cooperative Osteosarcoma Study group (COSS) patients. *J Clin Oncol*. 2020;38(8):823—833.
7. Bathaie SZ, Ashrafi M, Azizian M, Tamanoi F. Mevalonate pathway and human cancers. *Curr Mol Pharmacol*. 2017;10(2):77—85.
8. Mullen PJ, Yu R, Longo J, Archer MC, Penn LZ. The interplay between cell signalling and the mevalonate pathway in cancer. *Nat Rev Cancer*. 2016;16(11):718—731.
9. Brindisi M, Fiorillo M, Frattaruolo L, Sotgia F, Lisanti MP, Cappello AR. Cholesterol and mevalonate: two metabolites involved in breast cancer progression and drug resistance through the ERRα pathway. *Cells*. 2020;9(8):E1819.
10. Gupta VK, Sharma NS, Kesh K, et al. Metastasis and chemoresistance in CD133 expressing pancreatic cancer cells are dependent on their lipid raft integrity. *Cancer Lett*. 2018;439:101—112.
11. Kany S, Woschek M, Kneip N, et al. Simvastatin exerts anticancer effects in osteosarcoma cell lines via geranylgeranylation and c-Jun activation. *Int J Oncol*. 2018;52(4):1285—1294.
12. Zheng Y, Pan D. The Hippo signaling pathway in development and disease. *Dev Cell*. 2019;50(3):264—282.
13. Koohestanimobarhan S, Salami S, Imeni V, Mohammadi Z, Bayat O. Lipophilic statins antagonistically alter the major epithelial-to-mesenchymal transition signaling pathways in breast cancer stem-like cells via inhibition of the mevalonate pathway. *J Cell Biochem*. 2019;120(2):2515—2531.
14. Fullenkamp CA, Hall SL, Jaber OI, et al. TAZ and YAP are frequently activated oncoproteins in sarcomas. *Oncotarget*. 2016;7(21):30094—30108.
15. Li C, Wu W, Xie K, Feng Y, Xie N, Chen X. HMGCR is upregulated in gastric cancer and promotes the growth and migration of the cancer cells. *Gene*. 2016;587(1):42—47.
16. Göbel A, Breining D, Rauner M, Hofbauer LC, Rachner TD. Induction of 3-hydroxy-3-methylglutaryl-CoA reductase mediates statin resistance in breast cancer cells. *Cell Death Dis*. 2019;10(2):91.
17. Longo J, Mullen PJ, Yu R, et al. An actionable sterol-regulated feedback loop modulates statin sensitivity in prostate cancer. *Mol Metab*. 2019;25:119—130.
18. Ahmadi Y, Ghorbanihaghjo A, Argani H. The balance between induction and inhibition of mevalonate pathway regulates cancer suppression by statins: a review of molecular mechanisms. *Chem Biol Interact*. 2017;273:273—285.
19. Göbel A, Rauner M, Hofbauer LC, Rachner TD. Cholesterol and beyond - the role of the mevalonate pathway in cancer biology. *BBA Rev Cancer*. 2020;1873(2):188351.
20. Sorrentino G, Ruggeri N, Specchia V, et al. Metabolic control of YAP and TAZ by the mevalonate pathway. *Nat Cell Biol*. 2014;16(4):357—366.
21. Sethunath V, Hu H, De Angelis C, et al. Targeting the mevalonate pathway to overcome acquired anti-HER2 treatment resistance in breast cancer. *Mol Cancer Res*. 2019;17(11):2318—2330.
22. Zanconato F, Cordenonsi M, Piccolo S. YAP/TAZ at the Roots of Cancer. *Cancer Cell*. 2016;29(6):783—803.
23. Collak FK, Demir U, Ozkanli S, Kurum E, Zerk PE. Increased expression of YAP1 in prostate cancer correlates with extraprostatic extension. *Cancer Biol Med*. 2017;14(4):405—413.
24. Cao L, Sun PL, Yao M, Jia M, Gao H. Expression of YES-associated protein (YAP) and its clinical significance in breast cancer tissues. *Hum Pathol*. 2017;68:166—174.
25. Xia Y, Chang T, Wang Y, et al. YAP promotes ovarian cancer cell tumorigenesis and is indicative of a poor prognosis for ovarian cancer patients. *PloS One*. 2014;9(3), e91770.

26. He C, Mao D, Hua G, et al. The Hippo/YAP pathway interacts with EGFR signaling and HPV oncoproteins to regulate cervical cancer progression. *EMBO Mol Med*. 2015;7(11):1426—1449.
27. Dong L, Lin F, Wu W, Liu Y. Verteporfin inhibits YAP-induced bladder cancer cell growth and invasion via Hippo signaling pathway. *Int J Med Sci*. 2018;15(6):645—652.
28. Nguyen LT, Tretiakova MS, Silvis MR, et al. ERG activates the YAP1 transcriptional program and induces the development of age-related prostate tumors. *Cancer Cell*. 2015;27(6):797—808.
29. Zhang YH, Li B, Shen L, Shen Y, Chen XD. The role and clinical significance of Yes-associated protein 1 in human osteosarcoma. *Int J Immunopathol Pharmacol*. 2013;26(1):157—167.
30. Chan LH, Wang W, Yeung W, Deng Y, Yuan P, Mak KK. Hedgehog signaling induces osteosarcoma development through Yap1 and H19 overexpression. *Oncogene*. 2014;33(40):4857—4866.
31. Santinon G, Pocaterra A, Dupont S. Control of YAP/TAZ activity by metabolic and nutrient-sensing pathways. *Trends Cell Biol*. 2016;26(4):289—299.
32. Zhang X, Zhao H, Li Y, et al. The role of YAP/TAZ activity in cancer metabolic reprogramming. *Mol Cancer*. 2018;17(1):134.
33. Ji L, Liu C, Yuan Y, et al. Key roles of Rho GTPases, YAP, and *mutant p53* in anti-neoplastic effects of statins. *Fundam Clin Pharmacol*. 2020;34(1):4—10.
34. Liu Q, Xia H, Zhou S, et al. Simvastatin Inhibits the malignant behaviors of gastric cancer cells by simultaneously suppressing YAP and β-catenin signaling. *Oncotargets Ther*. 2020;13:2057—2066.
35. Wang Z, Wu Y, Wang H, et al. Interplay of mevalonate and Hippo pathways regulates RHAMM transcription via YAP to modulate breast cancer cell motility. *Proc Natl Acad Sci USA*. 2014;111(1):E89—E98.
36. Karlic H, Thaler R, Gerner C, et al. Inhibition of the mevalonate pathway affects epigenetic regulation in cancer cells. *Cancer Genet*. 2015;208(5):241—252.
37. Buhaescu I, Izzedine H. Mevalonate pathway: a review of clinical and therapeutical implications. *Clin Biochem*. 2007;40(9—10):575—584.
38. Likus W, Siemianowicz K, Bieńk K, et al. Could drugs inhibiting the mevalonate pathway also target cancer stem cells? *Drug Resist Updat*. 2016;25:13—25.
39. Elsayed M, Kobayashi D, Kubota T, et al. Synergistic antiproliferative effects of zoledronic acid and fluvastatin on human pancreatic cancer cell lines: an in vitro study. *Biol Pharm Bull*. 2016;39(8):1238—1246.
40. Göbel A, Thiele S, Browne AJ, et al. Combined inhibition of the mevalonate pathway with statins and zoledronic acid potentiates their anti-tumor effects in human breast cancer cells. *Cancer Lett*. 2016;375(1):162—171.
41. Ungefroren H, Witte D, Lehnert H. The role of small GTPases of the Rho/Rac family in TGF-β-induced EMT and cell motility in cancer. *Dev Dyn*. 2018;247(3):451—461.
42. Struckhoff AP, Rana MK, Worthylake RA. RhoA can lead the way in tumor cell invasion and metastasis. *Front Biosci (Landmark Ed)*. 2011;16:1915—1926.
43. Zaoui K, Boudhraa Z, Khalifé P, Carmona E, Provencher D, Mes-Masson AM. Ran promotes membrane targeting and stabilization of RhoA to orchestrate ovarian cancer cell invasion. *Nat Commun*. 2019;10(1):2666.
44. Kim YN, Choe SR, Cho KH, et al. Resveratrol suppresses breast cancer cell invasion by inactivating a RhoA/YAP signaling axis. *Exp Mol Med*. 2017;49(2):e296.